Refraction of a surface polariton by an interface

G. I. Stegeman,* A. A. Maradudin, and T. S. Rahman
Department of Physics, University of California, Irvine, California 92717
(Received 29 September 1980)

By means of a normal-mode analysis, transmission and reflection coefficients have been calculated for a surface polariton crossing a plane boundary at normal incidence from one surface-active medium to another. The energy radiated into the vacuum above the two surface-active media has also been calculated.

I. INTRODUCTION

In recent years considerable interest has arisen in the study of surface polaritons.[1] These are electromagnetic waves that propagate along the surface of a dielectric medium and whose amplitudes decay exponentially with increasing distance from the surface. The recent studies have focused primarily on surface polaritons with frequencies in the infrared, where a variety of resonances in the dielectric (or magnetic) response of the substrate can lead to the satisfaction of the conditions required for surface-polariton propagation.

In the recent studies of these waves much attention has been given to methods of generating them and to the study of their dispersion relation. Their attenuation has been studied both experimentally[2] and theoretically,[3] and recently the nonlinear interactions of surface polaritons have been studied theoretically[4] and experimentally.[5]

One can now envision optical circuits impressed on surfaces over which surface polaritons propagate, rather similar in nature to those employed in the field of integrated optics. To assess the effectiveness of such a circuit a study of one basic phenomenon is required. This is the refraction of a surface polariton by an interface encountered by it.

In this paper we study this phenomenon for an elementary geometry exhibiting it (Fig. 1). The surface lies in the x_1x_2 plane. The region $0 < x_3 < d_0$ is vacuum. The region $x_1 < 0$, $-d < x_3 < 0$ is occupied by a surface-active dielectric medium characterized by a real scalar, frequency-dependent dielectric constant $\epsilon_1(\omega)$; the region $x_1 > 0$, $-d < x_3 < 0$ is occupied by a second, surface-active dielectric medium, characterized by a real dielectric constant $\epsilon_2(\omega)$. (A surface-active medium is one that supports surface-polariton propagation, when it is in contact with vacuum, in the frequency range of interest.) The planes $x_3 = d_0$ and $x_3 = -d$ are metallized, which serves to ground the tangential components of the electric fields at these surfaces.

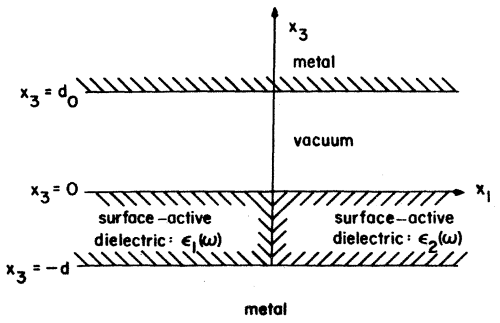

FIG. 1. The structure studied in this paper.

The structure depicted in Fig. 1 supports surface-polariton propagation for both $x_1 < 0$ and $x_1 > 0$. A surface wave incident on the interface at the plane $x_1 = 0$ from the left will be partially reflected from the interface, and there will be a transmitted surface wave as well.

The problem we consider here is that of calculating the amplitudes of the reflected and transmitted surface waves, and from them the transmission and reflection coefficients when the incident surface polariton propagates normally to the interface at the plane $x_1 = 0$, i.e., along the x_1 axis. The case of non-normal incidence will be considered in a separate publication. The problem is complicated by the fact that the depth attenuation constants of a surface polariton in the region $x_1 < 0$ differ from those of a surface polariton in the region $x_1 > 0$. Consequently, the boundary conditions on the electromagnetic fields at the interface $x_1 = 0$ cannot be satisfied by matching surface waves alone across this interface. It is necessary to admix radiative waves into the solutions in the two regions $x_1 < 0$ and $x_1 > 0$ as well. This shows that when the incident surface polariton strikes the interface it loses a portion of its energy to waves radiated away from the interface into the vacuum. Consequently, the sum of the energies in the reflected and transmitted surface waves is less than the energy in the incident surface polariton. In this paper, we calculate the reflection and transmission coefficients of the surface polariton, and the radiative losses, by expanding the electromag-

netic fields in the structure of Fig. 1 in terms of the normal modes of the structure for each of the regions $x_1<0$ and $x_1>0$.

A word is in order here concerning our use of the confined geometry depicted in Fig. 1 for obtaining the transmission and reflection coefficients for a surface polariton. In earlier work on this problem[6] we used a semi-infinite system that is obtained from the one shown in Fig. 1 by removing the upper metallized boundary at $x_3=d_0$. The normal-mode expansion used was the one introduced by Shevchenko[7] and used in a context similar to that of the present work by Mahmoud and Beal.[8] However, it proved impossible by that approach to obtain the kind of numerical accuracy, in particular for the conservation of energy, that we have been able to achieve in the present work. In Sec. III we present some results that suggest that our results for the transmission and reflection coefficient are not very sensitive to our use of a finite value of d_0.

II. NORMAL-MODE ANALYSIS

We start by obtaining the electromagnetic modes of the two-layer structure consisting of vacuum in the region $0<x_3<d_0$, a dielectric film characterized by a real, isotropic, frequency-dependent dielectric constant $\epsilon(\omega)$ in the region $-d<x_3<0$, with the surfaces $x_3=d_0$ and $x_3=-d$ metallized. We seek solutions of Maxwell's equations in the form of p-polarized waves given by

$$\vec{E}(\vec{x},t)=[\hat{x}_1 E_1(x_1x_3|\,\omega)+\hat{x}_3 E_3(x_1x_3|\,\omega)]e^{-i\omega t}, \quad (2.1a)$$

$$\vec{H}(\vec{x},t)=\hat{x}_2 H_2(x_1x_3|\,\omega)e^{-i\omega t}, \quad (2.1b)$$

where $\hat{x}_1,\hat{x}_2,\hat{x}_3$ are unit vectors in the 1, 2, 3 directions, respectively. The solutions for $E_1(x_1x_3|\,w)$, $E_3(x_1x_3|\,\omega)$, and $H_2(x_1x_3|\,\omega)$ that satisfy the requirements that $E_1(\vec{x},t)$ and $H_2(\vec{x},t)$ be continuous across the plane $x_3=0$, and that $E_1(\vec{x},t)$ vanish at $x_3=d_0$ and at $x_3=-d$, are

$$E_1(x_1x_3|\,\omega)=\begin{cases}\dfrac{ic\alpha_0}{\omega}\dfrac{\sinh\alpha_0(d_0-x_3)}{\cosh\alpha_0 d_0}e^{i\beta x_1}, & 0<x_3<d_0 \quad (2.2a)\\ -\dfrac{ic\alpha}{\omega\epsilon(\omega)}\dfrac{\sinh\alpha(d+x_3)}{\cosh\alpha d}e^{i\beta x_1}, & -d<x_3<0 \quad (2.2b)\end{cases}$$

$$E_3(x_1x_3|\,\omega)=\begin{cases}-\dfrac{c\beta}{w}\dfrac{\cosh\alpha_0(d_0-x_3)}{\cosh\alpha_0 d_0}e^{i\beta x_1}, & 0<x_3<d_0 \quad (2.3a)\\ -\dfrac{c\beta}{\omega\epsilon(\omega)}\dfrac{\cosh\alpha(d+x_3)}{\cosh\alpha d}e^{i\beta x_1}, & -d<x_3<0 \quad (2.3b)\end{cases}$$

$$H_2(x_1x_3|\,\omega)=\begin{cases}\dfrac{\cosh\alpha_0(d_0-x_3)}{\cosh\alpha_0 d_0}e^{i\beta x_1}, & 0<x_3<d_0 \quad (2.4a)\\ \dfrac{\cosh\alpha(d+x_3)}{\cosh\alpha d}e^{i\beta x_1}, & -d<x_3<0 \quad (2.4b)\end{cases}$$

In Eqs. (2.2)–(2.4) c is the speed of light, and the functions $\alpha_0(\beta\omega)$ and $\alpha(\beta\omega)$ are defined by

$$\alpha_0(\beta\omega)=\left(\beta^2-\frac{\omega^2}{c^2}\right)^{1/2}, \quad \mathrm{Re}\alpha_0>0,\ \mathrm{Im}\alpha_0>0 \quad (2.5a)$$

$$\alpha(\beta\omega)=\left(\beta^2-\epsilon(\omega)\frac{\omega^2}{c^2}\right)^{1/2}, \quad \mathrm{Re}\alpha>0,\ \mathrm{Im}\alpha>0. \quad (2.5b)$$

For a given value of the frequency ω, the allowed values of β for which the modes (2.2) – (2.4) are defined are the solutions of the dispersion relation

$$\epsilon(\omega)\frac{\alpha_0(\beta\omega)}{\alpha(\beta\omega)}=-\frac{\tanh\alpha(\beta\omega)d}{\tanh\alpha_0(\beta\omega)d_0}. \quad (2.6)$$

The solutions of this equation are discrete and are labeled by a double index $(i)m$, where $i=1,2$ indicates which dielectric constant $\epsilon_1(\omega)$ or $\epsilon_2(\omega)$ appears in Eq. (2.6), and m labels the solutions for a given $\epsilon(\omega)$. The solutions of Eq. (2.6) are complex in general,

$$\beta=\beta_1+i\beta_2, \quad (2.7a)$$

where

$$\beta_1>0, \quad \beta_2>0, \quad (2.7b)$$

for a wave that propagates in the $+x_1$ direction or decays exponentially with increasing x_1.

Modes are ordered in the order of decreasing β_1 until $\beta_1=0$, then according to increasing β_2. The value of β corresponding to the surface polariton is real, and we denote it by β_0.

Thus, we label the normal modes (2.2)–(2.4) by a double index $(i)m$, corresponding to the value of $\beta=\beta_{(i)m}$ for which they are evaluated. Modes for $x_1<0$ are denoted by, e.g., ${}^{(1)}E_\alpha^{(m)}(x_1x_3|\,\omega)$; modes for $x_1<0$ are denoted by, e.g., ${}^{(2)}E_\alpha^{(m)}(x_1x_3|\,\omega)$. Modes for which β is replaced by $-\beta$, corresponding to reflected waves, are denoted by a bar over the corresponding symbols for the field components.

We can now write the components of the electromagnetic field in each of the regions $x_1<0$ and $x_1>0$ as expansions in the corresponding normal modes.

For $x_1<0$:

$$\vec{E}^{<}(\vec{x},t)=[\hat{x}_1\mathcal{E}_1^{<}(x_1x_3|\,\omega)+\hat{x}_3\mathcal{E}_3^{<}(x_1x_3|\,\omega)]e^{-i\omega t}, \quad (2.8a)$$

$$\vec{H}^{<}(x,t)=\hat{x}_2\mathcal{H}_2^{<}(x_1x_3|\,\omega)e^{-i\omega t}, \tag{2.8b}$$

where

$$\mathcal{E}_1^{<}(x_1x_3|\,\omega)={}^{(1)}E_1^{(0)}(x_1x_3|\,\omega)+r\,{}^{(1)}E_1^{(0)}(x_1x_3|\,\omega)+\sum_{m(>0)}R_m\,{}^{(1)}E_1^{(m)}(x_1x_3|\,\omega), \tag{2.9a}$$

$$\mathcal{E}_3^{<}(x_1x_3|\,\omega)={}^{(1)}E_3^{(0)}(x_1x_3|\,\omega)+r\,{}^{(1)}E_3^{(0)}(x_1x_3|\,w)+\sum_{m(>0)}R_m\,{}^{(1)}E_3^{(m)}(x_1x_3|\,\omega), \tag{2.9b}$$

$$\mathcal{H}_2^{<}(x_1x_3|\,w)={}^{(1)}H_2^{(0)}(x_1x_3|\,\omega)+r\,{}^{(1)}H_2^{(0)}(x_1x_3|\,\omega)+\sum_{m(>0)}R_m\,{}^{(1)}H_2^{(m)}(x_1x_3|\,\omega). \tag{2.9c}$$

For $x_1>0$:

$$\vec{E}^{>}(\vec{x},t)=[\hat{x}_1\mathcal{E}_1^{>}(x_1x_3|\,\omega)+\hat{x}_3\mathcal{E}_3^{>}(x_1x_3|\,\omega)]e^{-i\omega t}, \tag{2.10a}$$

$$\vec{H}^{>}(\vec{x},t)=\hat{x}_2\mathcal{H}_2^{>}(x_1x_3|\,\omega)e^{-i\omega t}, \tag{2.10b}$$

where

$$\mathcal{E}_1^{>}(x_1x_3|\,\omega)=t\,{}^{(2)}E_1^{(0)}(x_1x_3|\,\omega)+\sum_{m(>0)}T_m\,{}^{(2)}E_1^{(m)}(x_1x_3|\,\omega), \tag{2.11a}$$

$$\mathcal{E}_3^{>}(x_1x_3|\,\omega)=t\,{}^{(2)}E_3^{(0)}(x_1x_3|\,\omega)+\sum_{m(>0)}T_m\,{}^{(2)}E_3^{(m)}(x_1x_3|\,\omega), \tag{2.11b}$$

$$\mathcal{H}_2^{>}(x_1x_3|\,\omega)=t\,{}^{(2)}H_2^{(0)}(x_1x_3|\,\omega)+\sum_{m(>0)}T_m\,{}^{(2)}H_2^{(m)}(x_1x_3|\,\omega). \tag{2.11c}$$

The coefficients r and t are the amplitudes of the reflected and transmitted surface polariton, respectively; R_m and T_m are the amplitudes of the mth reflected and transmitted modes other than the surface polariton. These include purely radiative vacuum modes (real β) and modes that decay exponentially with increasing $|x_1|$ (complex or pure imaginary β).

These coefficients are determined from the boundary conditions at the interface $x_1=0$. The two independent boundary conditions in the present problem are the continuity of $H_2(\vec{x},t)$ and $E_3(\vec{x},t)$ across this surface. The equations expressing these conditions are

$${}^{(1)}H_2^{(0)}(0x_3|\,\omega)+r\,{}^{(1)}H_2^{(0)}(0x_3|\,\omega)+\sum_{m(>0)}R_m\,{}^{(1)}H^{(m)}(0x_3|\,\omega)=t\,{}^{(2)}H_2^{(0)}(0x_3|\,\omega)+\sum_{m(>0)}T_m\,{}^{(2)}H_2^{(m)}(0x_3|\,\omega), \tag{2.12a}$$

$${}^{(1)}E_3^{(0)}(0x_3|\,\omega)+r\,{}^{(1)}E_3^{(0)}(0x_3|\,\omega)+\sum_{m(>0)}R_m\,{}^{(1)}E_3^{(m)}(0x_3|\,\omega)=t\,{}^{(2)}E_3^{(0)}(0x_3|\,\omega)+\sum_{m(>0)}T_m\,{}^{(2)}E_3^{(m)}(0x_3|\,\omega). \tag{2.12b}$$

The time-averaged power flow in the x_1 direction per unit width of the structure in Fig. 1 in the x_2 direction for a given mode can be expressed as

$$P_1=P_1^{>}+P_1^{<}, \tag{2.13}$$

where

$$P_1^{>}=-\frac{c}{8\pi}\,\mathrm{Re}\int_0^{d_0}dx_3E_3(x_1x_3|\,\omega)H_2^{*}(x_1x_3|\,\omega)=\frac{c^2\beta}{16\pi\omega}\frac{1}{|\cosh\alpha_0d_0|^2}\times\left(\frac{\sinh(\alpha_0+\alpha_0^{*})d_0}{\alpha_0+\alpha_0^{*}}+\frac{\sinh(\alpha_0-\alpha_0^{*})d_0}{\alpha_0-\alpha_0^{*}}\right), \tag{2.14a}$$

$$P_1^{<}=-\frac{c}{8\pi}\,\mathrm{Re}\int_{-d}^{0}dx_3E_e(x_1x_3|\,\omega)H_2^{*}(x_1x_3|\,\omega)=\frac{c^2\beta}{16\pi\omega\epsilon(\omega)}\frac{1}{|\cosh\alpha d|^2}\times\left(\frac{\sinh(\alpha+\alpha^{*})d}{\alpha+\alpha^{*}}+\frac{\sinh(\alpha-\alpha^{*})d}{\alpha-\alpha^{*}}\right). \tag{2.14b}$$

These expressions are nonzero only for those modes for which β is real. The quantity $P_1^{>}$ is the power flow in the vacuum, while $P_1^{<}$ is the power flow in the dielectric medium. Note that because $\epsilon(\omega)$ is negative at the frequency of a surface polariton the power flow in the dielectric medium is in the direction opposite to the direction of propagation of the surface wave.

The transmission and reflection coefficients for the surface polariton were obtained from these results by normalizing the power flow per unit width in the transmitted and reflected surface polaritons by that for the incident surface polariton. The energy carried by the vacuum modes will be normalized in the same way.

III. NUMERICAL RESULTS

In the present work the two distances d_0 and d were chosen to be equal. The surface-polariton reflection-transmission problem was investigated by satisfying the electromagnetic boundary conditions at a discrete number of points along the interface between the two media. A total of 52 equally spaced points were used, 26 along the vacuum portion of the interface and 26 on the boundary between the polariton active media. The tangential fields E_3 and H_2 were made continuous

at each of these points by using a superposition of 104 normal modes of the system, i.e., the amplitudes and phases of the modes were adjusted to enforce these continuity conditions. In the present case we chose 52 modes from each side of the boundary. This led to reasonable results since the mode spacing (as a function of β) depends primarily on the height dimension d, and varies only weakly with the magnitude of $\epsilon(\omega)$, i.e., the β's of the final modes in both media were of comparable value.

The model chosen to parametrize $\epsilon(\omega)$ was that of a free-electron gas. [The results, however, are valid for any model that produces the same values of $\epsilon(\omega)$.] Thus $\epsilon(\omega)=1-\omega_p^2/\omega^2$, where ω_p is the plasma frequency and ω is the surface-polariton frequency chosen so that $\epsilon(\omega)<1$, which is the range of existence for surface polaritons at the boundary between a semi-infinite dielectric medium and a semi-infinite vacuum. In the calculations we varied the ratio ω_p/ω by fixing ω $(=c)=1$ and changing ω_p. The height dimension was chosen to be the same in all media and was varied from 0.5 to 4.5 in units of $2\pi c/\omega$, and ω_p was varied from 1.5 to 4.8, corresponding to $\epsilon=-1.25$ and -22.04, respectively. Not all combinations of the above parameters could be studied for reasons of numerical nonsatisfaction of energy conservation, as will be discussed later.

The normal modes used were solutions of the dispersion relation, Eq. (2.6). Three types of modes were found that were characterized by real values of β, imaginary β, and complex β. For all values of d there always occurred at least one propagating mode solution (real β). The lowest-order solution was characterized by fields that decay exponentially away from the vacuum-polariton active medium boundary. It degenerates into a surface polariton at the boundary between two semi-infinite media in the limit $d\to\infty$ [as can be seen from Eq. (2.6)]. The values of β (as functions of ω_p/ω) for this lowest-order mode always lie above their values for $d\to\infty$. An example of this, for $d=1$, is shown in Fig. 2. Differences between the values of β for finite values of d and for $d\to\infty$ occur when the field in the vacuum would have had an appreciable value of $x_3=d$ had it not been "shorted out" by the metal plane. At $d=4.0$ the two curves become indistinguishable on the scale of Fig. 2. As d increases from zero, successively more modes that have a propagating nature in the vacuum (real wave vector) and are evanescent in the polariton active medium emerge. Owing to the presence of the "shorting" planes at $x_3=\pm d$, these vacuum modes appear as standing waves and the net energy transported by them is along the $\pm x_1$ directions. For the thickness range $n-0.2\lesssim d\lesssim n+0.8$ where n is a natural number $(n>1)$, there are n vacuum modes for each value of ω_p/ω. In our case, up to four such modes, i.e., a total of five propagating modes, including the polariton, occurred. The remaining (majority of the) modes used in the boundary condition problem were nonpropagating and decayed in an exponential fashion (along x_1) away from the boundary into each medium.

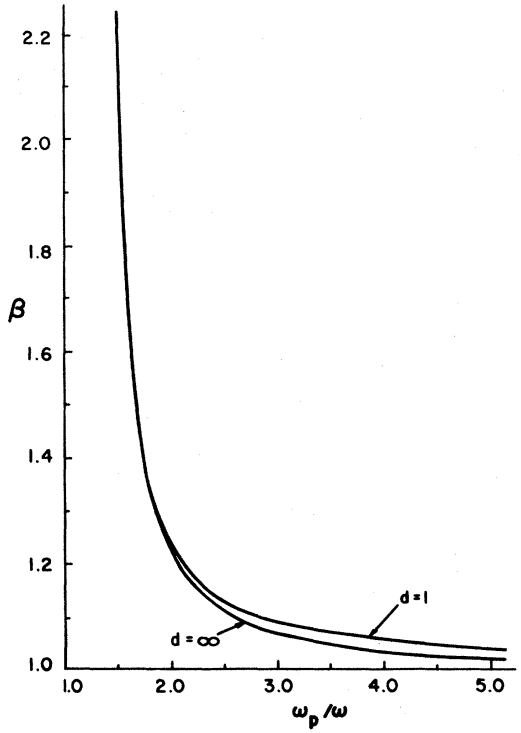

FIG. 2. The propagation constant β for the surface polariton as a function of ω_p/ω for two different values of the half-width d $(=d_0)$ of the structure in Fig. 1.

The procedure of matching the boundary conditions always ensures that they are satisfied at each of the discrete set of points. It, however, does not guarantee that they are also satisfied elsewhere. The criterion used to check the validity of the solutions was energy conservation, i.e., the total energy that appears in the reflected and transmitted propagating modes (real β) must equal the incident surface-polariton energy. In our calculations, the solutions were deemed acceptable when the ratio of the former energy to the latter was within 1.000 ± 0.005; in the best cases the discrepancy was as small as $\pm0.000\,01$. Convergence of the solutions (in terms of energy conservation) deteriorated both with increasing d and increasing difference between the ω_p/ω characteristic of the two media. The discrepancy from full energy conservation places an upper limit on the accuracy of

the numerical results for the mode energies, etc. Actually, we found the accuracy and reproducibility (with small changes in the number of subdivision points) of the mode energies to be much better than indicated by this limit when all of the results were scaled to complete energy conservation. For example, if for a particular case the conservation coefficient was 0.999, then the accuracy of all of the mode energies could be improved by dividing them all by 0.999 and hence scaling to unity the energy conservation. This feature was verified by varying the number of subdivision points, ω_p/ω, and d. Energy conservation proved to be very sensitive to the completeness of the set of the first 52 modes used for a given material; if a mode was missing, especially from the first 15–20 modes, large deviations from unity were obtained. There also occurred a small number of cases where two (in a set of 52) modes were almost degenerate and energy conservation could not be obtained to the desired accuracy.

The largest range of change in $\epsilon(\omega)$ (and ω_p/ω) between adjacent media was investigated for $d = 1.0$. The numerical results are summarized in Figs. 3 and 4. (Note that we quote energy rather than amplitude coefficients since the energy normalization varies dramatically from mode to mode.) Perhaps the most surprising aspect of the numerical results in the large fraction of the incident energy that is transmitted through the boundary, i.e.,

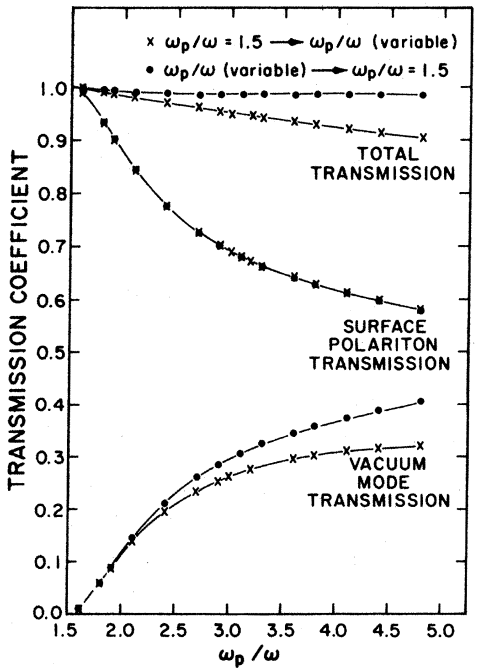

FIG. 3. Energy transmission coefficients for surface polaritons and vacuum modes for $d = 1.0$.

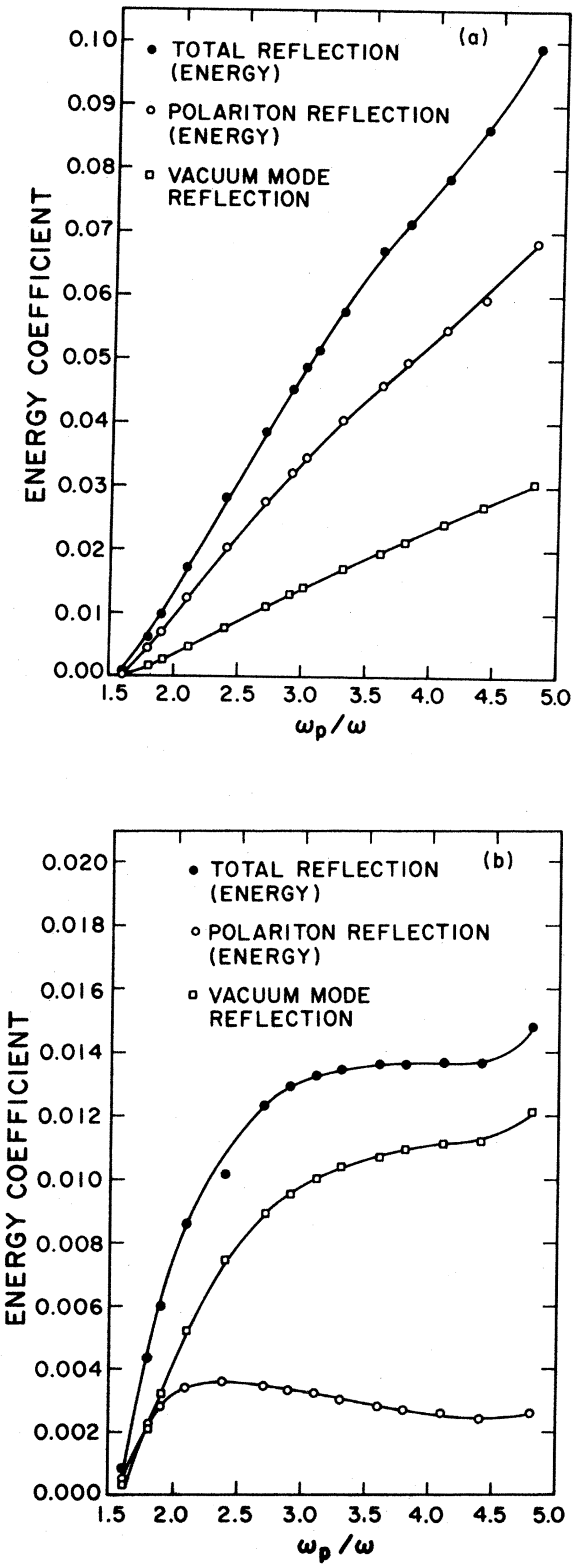

FIG. 4. Energy reflection coefficients for surface polaritons and vacuum modes for $d = 1.0$. (a) $\omega_p/\omega = 1.5 \rightarrow \omega_p/\omega$ (variable); (b) ω_p/ω (variable) $\rightarrow \omega_p/\omega = 1.5$.

the total fraction of energy transmitted in the form of propagating modes traveling along x_1. For the extreme case of a surface polariton propagating from a medium with $\epsilon = -1.25$ to a medium with $\epsilon = -22.04$ (i.e., from a medium with $\omega_p/\omega = 1.5$ to a medium with $\omega_p/\omega = 4.8$), the total transmission and reflection coefficients were 0.904 and 0.096, respectively. In normal plane-wave optics, which involves a single reflected and a single transmitted wave, for an equivalent change in ϵ one would expect transmission and reflection coefficients of ~ 0.6 and ~ 0.4, respectively. On considering just the surface-polariton part of the transmitted and reflected energies, we obtain coefficients of ~ 0.58 and ~ 0.07: The transmission coefficient here is in more reasonable agreement with the plane-wave analog. For a surface polariton, the bulk of the energy is usually carried in the vacuum portion of the mode, and no discontinuity in material properties is encountered by this component of the mode. On the other hand, different modes are characterized by different spatial distributions on both sides of the boundary. Nevertheless, this lack of discontinuity in material properties in the region where most of the mode energy is present may be the deciding factor that produces the large transmission and small reflection coefficients.

Another salient feature obtained for a boundary between two specific media is that the surface-polariton transmission coefficient is independent of the direction of the incident surface polariton. This is clearly evident in Fig. 3 for $d = 1.0$. This was also verified numerically for a number of combinations of the parameters with d in the range between 0.5 and 4.0. On the other hand, no similar correlation was found for the surface-polariton reflection coefficient for the range of parameters investigated, i.e., the reflection coefficient dependent upon the direction of incidence. We do note that the reflection coefficient is comparable in magnitude to the energy carried by the vacuum modes, which are very few in number in our calculations. Hence, the present calculations may well have been performed for values of d too small to show a general result for the surface-polariton reflection coefficient. As another example of directional anisotropy, we found that, when the surface polariton was incident towards a medium of smaller ω_p/ω, the total transmitted energy was larger than for incidence onto media characterized by larger ω_p/ω.

Some of the other trends exhibited in Figs. 3 and 4 are not unexpected. As the change in ϵ between adjacent media increases, the total reflected energy increases and conversely the total transmitted energy decreases. Furthermore, the fraction of the transmitted energy which appears as vacuum modes increases relative to the surface polariton transmitted energy.

The variation in the various energy coefficients with increasing d is shown in Figs. 5 and 6 for surface polaritons incident onto a medium characterized by $\omega_p/\omega = 2.7$ from a medium with $\omega_p/\omega = 1.8$. The total energy (surface polariton + vacuum modes) reflected by and transmitted through the boundary changes little with increasing d (Figs. 5 and 6), with the exception of small regions of d ($\Delta d \sim 0.2$) characteristic of the appearance of a new propagating vacuum mode. A gradual decrease in the total transmitted energy with increasing number of vacuum modes is discernible (and likewise a corresponding increase in the re-

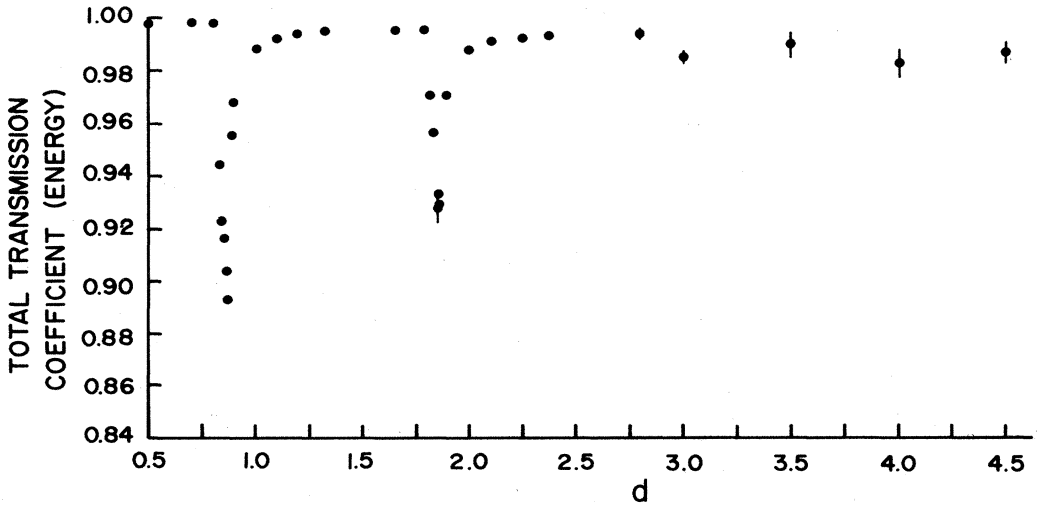

FIG. 5. Total energy transmission coefficient as a function of the half-width d ($= d_0$) of the structure in Fig. 1 for a surface polariton incident on a medium for which $\omega_p/\omega = 2.7$ from a medium for which $\omega_p/\omega = 1.8$.

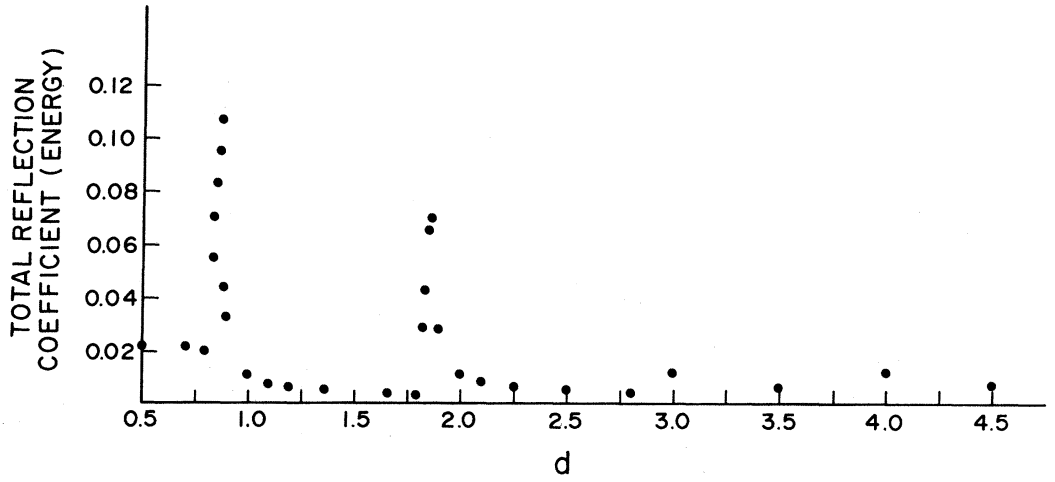

FIG. 6. Total energy reflection coefficient as a function of the half-width d $(=d_0)$ of the structure in Fig. 1 for a surface polariton incident on a medium for which $\omega_p/\omega=2.7$ from a medium for which $\omega_p/\omega=1.8$.

flected energy). Previous calculations on the reflection of Rayleigh waves at the end of a plate indicated that the reflection coefficient became independent of d after the number of propagating modes exceeded ~ 10.[9] Because of the similarity between the Rayleigh wave and surface-polariton problems, we would expect similar results in the present case. Hence the values for the total transmitted and reflected energies for $d>3.0$ probably provide reasonable estimates for the reflection-transmission problem for an interface between two semi-infinite media. This hypothesis is borne out effectively by the small changes in these energy coefficients, with increasing d.

The thickness dependence of just the surface-polariton transmission and reflection coefficients is shown in Figs. 7 and 8. As noted previously for the total energy coefficients, large variations in the surface-polariton reflection and transmission coefficients occurred in the vicinity of the emergence of new vacuum modes in the solution fields. However, for large d both coefficients are approximately independent of d, so that the limiting values of 0.90 for the transmission coefficient and 0.05 for the reflection coefficient should provide a reasonable estimate for the case of two semi-

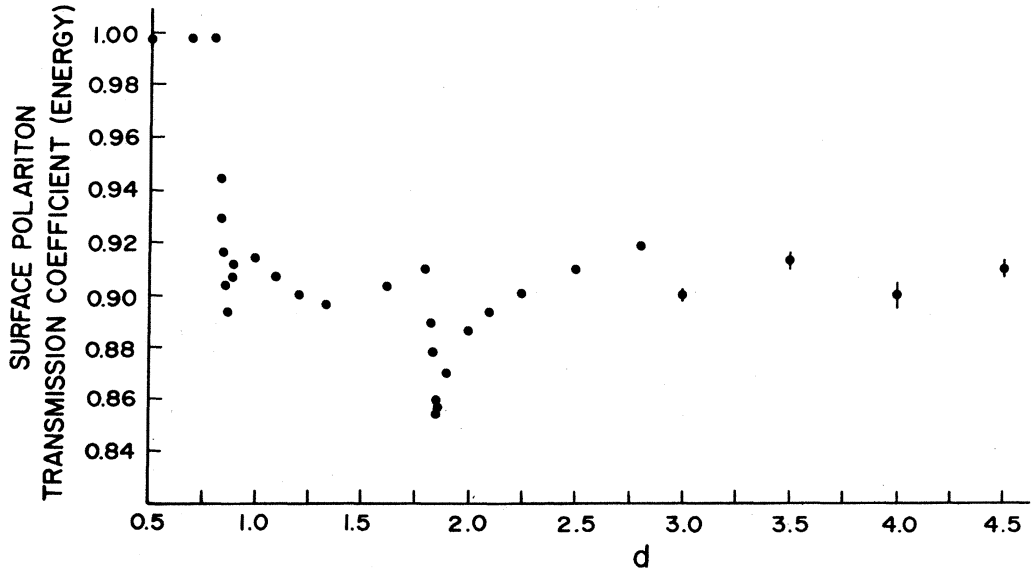

FIG. 7. The dependence of the surface-polariton transmission coefficient on the thickness of the half-width d $(=d_0)$ of the structure in Fig. 1 for a surface polariton incident on a medium for which $\omega_p/\omega=2.7$ from a medium for which $\omega_p/\omega=1.8$.

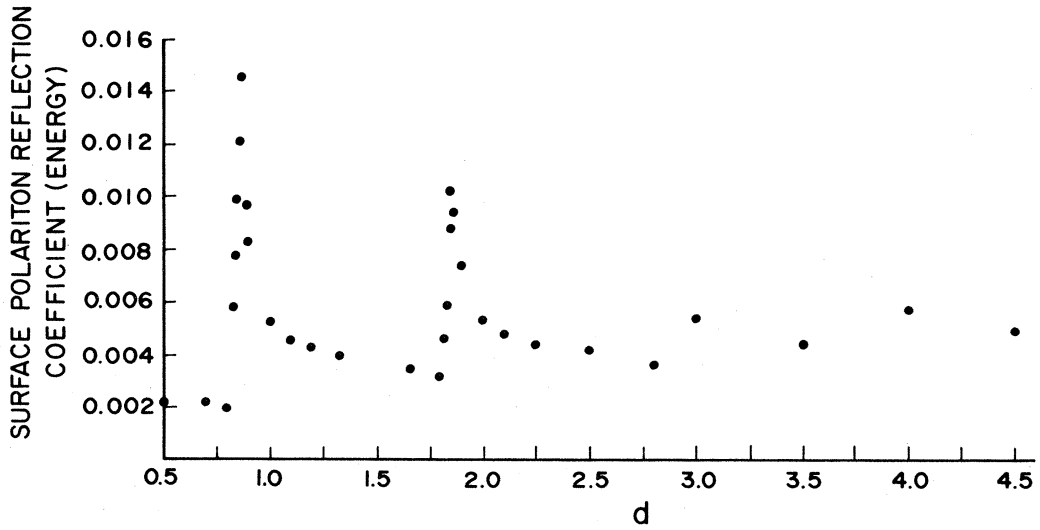

FIG. 8. The dependence of the surface-polariton reflection coefficient on the thickness of the half-width d $(=d_0)$ of the structure in Fig. 1 for a surface polariton incident on a medium for which $\omega_p/\omega=2.7$ from a medium for which $\omega_p/\omega=1.8$.

infinite media.

It is difficult to draw any definitive conclusion about the vacuum modes since our criterion for energy conservation did not allow investigation of cases with more than four such modes on each side of the boundary. Since both the total and surface-polariton reflected and transmitted energies are approximately independent of increases in d (for $d>3.0$), the energy that is converted into vacuum modes also becomes constant. The directions (for a limited number of discrete modes) into which the energy is radiated into the vacuum are shown in Figs. 9 and 10. Plotted there is the power generated along the direction of the total wave vector for one component of the standing waves that constitute the normal modes. In general, as in the case of the reflection of Rayleigh waves, very little energy is radiated into directions almost parallel to the media surfaces. Also evident from those diagrams is the large difference in the

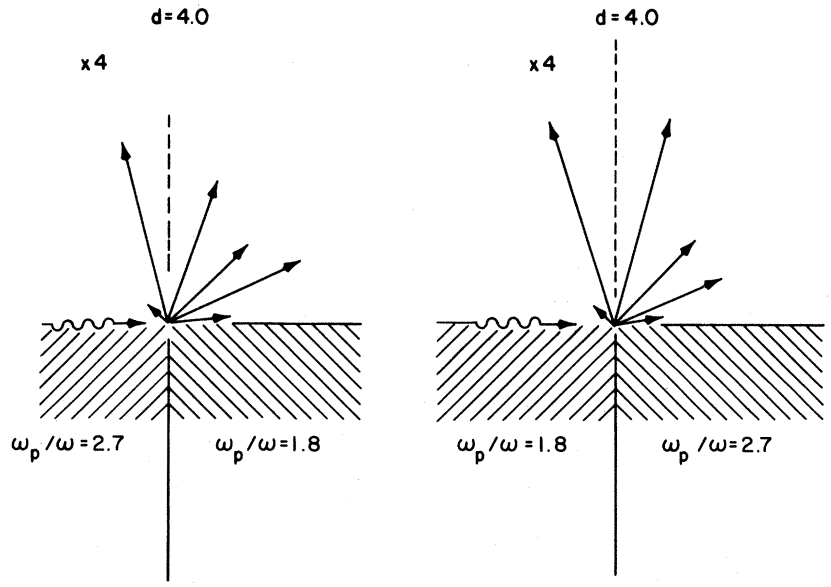

FIG. 9. The directions into which energy is radiated into the vacuum, for a limited number of vacuum modes. Plotted is the power generated along the direction of the total wave vector for one component of the standing waves that constitute the normal modes.

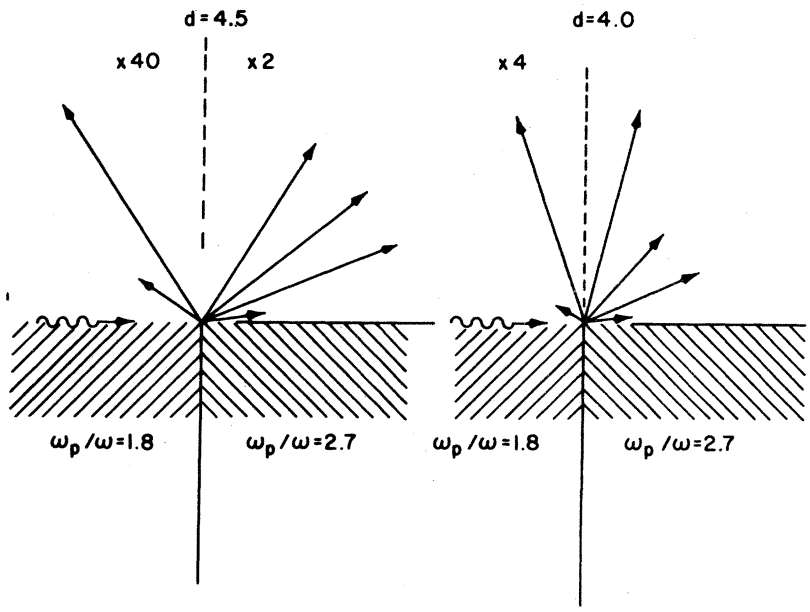

FIG. 10. The same as in Fig. 9.

energy radiated into the "transmitted" versus "reflected" directions. Although the results are certainly too sparse to be definitive, the power radiated seems to increase with angles away from the surfaces, again in agreement with the reflection of Rayleigh waves. In that case, the power radiated parallel to the interface ($\sim 90°$) from the media surfaces also falls to zero. In the present results there were no modes in approximately this direction and so this feature could not be tested. For the case in which the incident surface polaritons approach the boundary from opposite directions, the transmitted and reflected radiation patterns are similar in structure, but differ in the total power radiated.

Some additional general remarks about the usefulness of this discrete element approach to surface mode reflection and transmission problems might prove useful. In general, analytical solutions when available are always preferable. The problem with the present numerical approach is that it is difficult to identify the trends unambiguously: There is always the chance that the results may be representative only of the range of parameters studied. Furthermore, the ability of a discrete number of modes to reproduce a continuous field distribution accurately depends on how much the field changes in amplitude and phase between successive points along the boundary. In principle, the number of subdivisions (and superimposed normal modes) may be increased until the calculated fields are identical to the required field distribution to arbitrary accuracy. In practice this method relies on solving a set of $2n$ linear equations where n is the number of subdivisions used. This involves storing a matrix of $2n \times 2n$ coefficients and inverting it numerically. Hence the maximum number of points used is limited by a combination of the core memory storage available and the expense and accuracy (for large n) of inverting a complex $2n \times 2n$ matrix. In our case, this compromise led to a 104×104 matrix.

ACKNOWLEDGMENTS

We are thankful to Professor D. L. Mills for helpful comments on this calculation. This research was supported in part by AFOSR Grant No. F49620-78-C-0019.

*Present address: Optical Sciences Center, University of Arizona, Tucson, Arizona 85721

[1]See, for example, the review by E. Burstein, A. Hartstein, J. Schoenwald, A. A. Maradudin, D. L. Mills, and R. F. Wallis, in *Polaritons*, edited by E. Burstein and F. de Martini (Pergamon, New York, 1974), p. 89; D. L. Mills and E. Burstein, Rep. Prog. Phys. 37, 817 (1974); K. L. Kliewer and R. Fuchs, Adv. Chem. Phys. 27, 355 (1974).

[2]J. Schoenwald, E. Burstein, and J. Elson, Solid State Commun. 12, 185 (1973).

[3]D. L. Mills, Phys. Rev. B 12, 4036 (1975); A. A. Maradudin and W. Zierau, *ibid.* 14, 484 (1976).

[4]D. L. Mills, Solid State Commun. 24, 669 (1977);

M. Fukui and G. I. Stegeman, *ibid*. 26, 239 (1978); Lynn Bonsall and A. A. Maradudin, J. Appl. Phys. 49, 253 (1978).
[5]H. J. Simon, D. E. Mitchell, and J. G. Watson, Phys. Rev. Lett. 33, 1531 (1974).
[6]T. S. Rahman and A. A. Maradudin, Bull. Am. Phys. Soc. 23, 30 (1978).
[7]V. V. Shevchenko, *Continuous Transitions in Open Waveguides* (Golem, Boulder, Colorado, 1971).
[8]S. F. Mahmoud and J. C. Beal, IEEE Trans. Microwave Theory and Tech. MTT-23, 193 (1975).
[9]K. Portz, G. I. Stegeman, and A. A. Maradudin (unpublished).